DALTON
FULL PAPER

Copper(II) complexes of C-*meso*-1,5,8,12-tetramethyl-1,4,8,11-tetraazacyclotetradecane: syntheses, structures and properties†

Tian-Huey Lu,[a] Shih-Chi Lin,[b] Halikhedkar Aneetha,[b] Kaliyamoorthy Panneerselvam[a] and Chung-Sun Chung[b]

[a] *Department of Physics, National Tsing Hua University, Hsinchu, Taiwan 300, ROC*
[b] *Department of Chemistry, National Tsing Hua University, Hsinchu, Taiwan 300, ROC*

Received 24th June 1999, Accepted 10th August 1999

A series of copper(II) complexes of C-*meso*-1,5,8,12-tetramethyl-1,4,8,11-tetraazacyclotetradecane L^1 have been synthesized and characterized. The crystal structure of $[CuL^1(ClO_4)]ClO_4$ **1** showed the macrocyclic ligand in the unstable *trans*-II configuration, while those of $[CuL^1(N_3)_2]$ **2** and $[CuL^1(H_2O)_2]X_2$ (X = NO_2 **3**, Cl **4**, Br **5** or I **6**) showed the macrocyclic ligand to be in the stable *trans*-III configuration. The metal ion is in a tetragonally elongated octahedral geometry in all the complexes. In **1** one of the perchlorate groups is free while the other bridges two metal ions with two of its oxygen atoms thus forming a linear chain, while in **2** the axial positions are occupied by the nitrogen atoms of two azide groups. The complexes **3**–**6** are isomorphous. The electronic spectral and the redox properties of the complexes are discussed. The acid dissociation kinetics of **1** has been studied in the temperature range 25.0 ± 0.1 to 45 ± 0.1 °C in aqueous HNO_3–$NaNO_3$ solutions (I = 5.0 M). The complex exhibited a first order dependence on the hydrogen ion concentration with $k_{obs} = k_{1H}[H^+] + k_{1d}$ where $k_{1H} = 2.66 \times 10^{-5}$ M^{-1} s^{-1} and $k_{1d} = 5.54 \times 10^{-5}$ s^{-1} at 25.0 ± 0.1 °C. The temperature dependence of the rate constant for the reaction gave $\Delta H^{\ddagger}_{1H} = 64.7$ kJ mol^{-1} and $\Delta S^{\ddagger}_{1H} = -117$ J K^{-1} mol^{-1} for k_{1H} while for k_{1d} the parameters are $\Delta H^{\ddagger}_{1d} = 27.4$ kJ mol^{-1} and $\Delta S^{\ddagger}_{1d} = -234$ J K^{-1} mol^{-1}. A possible mechanism of the reaction is discussed.

The co-ordination chemistry of tetraaza macrocycles has been studied extensively.[1] Previously we have reported detailed dissociation kinetic studies of a few copper(II) complexes of 14-membered tetraaza macrocyclic complexes in strongly acidic aqueous media.[2–5] We have extended the studies to copper(II) complexes of di-*N*-alkylated tetraaza macrocycles. This paper reports syntheses, structures and properties of copper(II) complexes of C-*meso*-1,5,8,12-tetramethyl-1,4,8,11-tetraazacyclotetradecane, L^1. The crystal structures of complexes $[CuL^1(ClO_4)]ClO_4$ **1**, $[CuL^1(N_3)_2]$ **2**, $[CuL^1(H_2O)_2]X_2$ (X = NO_2 **3**, Cl **4**, Br **5** or I **6**) are reported. The acid dissociation kinetics of **1** has been studied in detail in aqueous HNO_3–$NaNO_3$ solutions. Interestingly in the present complex cleavage of the first Cu–N bond is the rate determining step, unlike in the other 14-membered tetraaza macrocyclic complexes reported previously where cleavage of the second Cu–N bond is the rate determining step. To the best of our knowledge, no detailed dissociation kinetic studies of di-*N*-methylated tetraaza macrocyclic complexes have been reported. The possible mechanism of the reaction, the factors influencing the rates and the relative importance of the protonation and solvation pathways are discussed.

Experimental

All the chemicals were of reagent grade and used without further purification. The ligand C-*meso*-1,5,8,12-tetramethyl-1,4,8,11-tetraazacyclotetradecane was synthesized by a reported procedure.[6] All the solvents were dried prior to use by standard procedures.[7]

†*Supplementary data available*: rotatable 3-D crystal structure diagram in CHIME format. See http://www.rsc.org/suppdata/dt/1999/3385/

Also available: electronic spectra showing the acid catalyzed dissociation of **1** in aqueous HNO_3–$NaNO_3$ solution (I = 5 M) at 25 ± 0.1 °C. Available from BLDSC (No. SUP 57621, 2 pp.). See Instructions for Authors, 1999, Issue 1 (http://www.rsc.org/dalton).

Syntheses of complexes

$[CuL^1(ClO_4)]ClO_4$ 1. Equimolar quantities of copper perchlorate hexahydrate and the ligand were mixed in methanol and the solution was heated under reflux for 2 h. It was then cooled to room temperature. The red solid that precipitated was separated by filtration. (The structure of this red isomer was reported recently by our group.[8]) The filtrate was evaporated to dryness to give a blue solid. Repeated recrystallization of this solid from methanol gave the pure blue isomer. Crystals were obtained by slow evaporation of the methanol solution, yield 27% (Found: C, 32.3; H, 6.1; N, 10.6. Calc. for $C_{14}H_{32}Cl_2CuN_4O_8$: C, 32.4; H, 6.2; N, 10.8%). IR (KBr, cm^{-1}): 3105 [ν(N–H)] and 1145 to 1100 [$\nu(ClO_4)$].

$[CuL^1(N_3)_2]$ 2. Copper(II) acetate monohydrate (0.06 g, 0.3 mmol), ligand (0.1 g, 0.22 mmol) and NaN_3 (0.05 g, 0.77 mmol) in methanol (30 cm^3) were heated to reflux for 2 h. The solution was filtered and the solvent volume reduced to 5 cm^3 on a rotary evaporator. Slow evaporation of this solution gave crystals suitable for X-ray crystallography, yield 85% (Found: C, 34.5; H, 8.0; N, 34.6. Calc. for $C_{14}H_{32}CuN_{10}$: C, 34.7; H, 8.0; N, 34.7%). IR (KBr, cm^{-1}): 3100 [ν(N–H)] and 2028 [ν(N≡N)].

$[CuL^1(H_2O)_2][NO_2]_2$ 3. This complex was prepared and recrystallized in the same way as **2** except $NaNO_2$ was used instead of NaN_3, yield 65% (Found: C, 37.3; H, 7.9; N, 18.6. Calc. for $C_{14}H_{36}CuN_6O_6$: C, 37.5; H, 8.1; N, 18.8%). IR (KBr, cm^{-1}): 3370 [ν(O–H)] and 3100 [ν(N–H)].

$[CuL^1(H_2O)_2]Cl_2$ 4. A mixture of copper acetate monohydrate (0.06 g, 0.3 mmol) and ligand (0.1 g, 0.22 mmol) was dissolved in methanol (30 cm^3) and refluxed for 2 h. Sodium chloride (0.05 g, 0.8 mmol) was added and heating continued for 1 h. The reaction mixture was filtered hot. The filtrate was reduced to small volume (*ca.* 2 cm^3) on a rotary evaporator. The blue solid obtained was recrystallized from 0.1 M HCl, yield

70% (Found: C, 39.2; H, 8.4; N, 13.1. Calc. for $C_{14}H_{36}Cl_2CuN_4O_2$: C, 39.4; H, 8.5; N, 13.1%). IR (KBr, cm^{-1}): 3355 [ν(O–H)] and 3090 [ν(N–H)].

$[CuL^1(H_2O)_2]Br_2$ 5 and $[CuL^1(H_2O)_2]I_2$ 6. These complexes were synthesized in the same way as **4** except NaBr or NaI respectively was added instead of NaCl. Complex **5** was recrystallized from 10% hydrobromic acid solution in methanol, yield 40% (Found: C, 32.4; H, 7.0; N, 10.6. Calc. for $C_{14}H_{36}Br_2CuN_4O_2$: C, 32.6; H, 7.0; N, 10.9%). IR (KBr, cm^{-1}): 3368 [ν(O–H)] and 3100 [ν(N–H)]. Complex **6** was recrystallized from methanol, yield 52% (Found: C, 27.5; H, 6.1; N, 9.0. Calc. for $C_{14}H_{36}CuI_2N_4O_2$: C, 27.6; H, 6.0; N, 9.2%). IR (KBr, cm^{-1}): 3390 [ν(O–H)] and 3105 [ν(N–H)].

Physical measurements

The carbon, hydrogen and nitrogen analyses were carried out on a Heraeus CHN elemental analyzer. Infrared spectra were recorded on a BOMEN (Hartmann-Braun MB series) FT-IR spectrophotometer as KBr pellets, electronic absorption spectra on a Hitachi U-3300 UV/VIS spectrophotometer. Cyclic voltammetric studies were carried out on a CH instruments, model 604A computer controlled electrochemical analyzer. All the experiments were performed under a dry nitrogen atmosphere in acetonitrile solvent using 0.1 M NBu_4ClO_4 as the supporting electrolyte. A three-electrode assembly comprising a platinum working electrode, a platinum auxiliary electrode and Ag–AgCl reference electrode was used. The ferrocene–ferrocenium couple was used as the redox standard.

Kinetic studies. Kinetic measurements for acid catalyzed dissociation reactions of complex **1** were carried out in aqueous HNO_3–$NaNO_3$ solutions of ionic strength 5.0 M in the temperature range of 25.0 ± 0.1 to 45.0 ± 0.1 °C. Absorbance *vs.* time data were collected at 538 nm using a Hitachi U-3300 spectrophotometer. Very good first order kinetics was observed and the rate constants were obtained by linear least squares fit using a computer.

Crystallography

Intensity data were collected either on an Enraf-Nonius CAD4 or Siemens SMART CCD diffractometer using graphite-monochromated Mo-Kα radiation ($\lambda = 0.71073$ Å). Cell constants were determined by a least-squares fit to the setting parameters of 25 independent reflections. Data reduction and empirical absorption corrections (ψ scans[9]) were performed with the XTAL package[10] or NRCVAX programs.[11] Crystals of complexes **1** and **5** suffered from poor diffraction quality and power and only mediocre quality data could be collected resulting in poor refinements.

Structures were solved by the heavy atom method with SHELXS 97[12] and refined by full matrix least-squares analysis on F^2 with SHELXL 97.[13] All the non-hydrogen atoms were refined anisotropically and the hydrogen atoms fixed at calculated positions and refined using a riding model. The important crystallographic parameters are given in Table 1.

CCDC reference number 186/1610.

See http://www.rsc.org/suppdata/dt/1999/3385/ for crystallographic files in .cif format.

Results and discussion

Syntheses

Reaction of L^1 with copper perchlorate in methanol gave a mixture of complexes. A red precipitate was obtained and separated by filtration.[8] Slow evaporation of the filtrate gave complex **1**, a blue isomer. Complexes **2** and **3** were synthesized by reaction of ligand and copper acetate in methanol in the presence of sodium azide and sodium nitrite respectively, while **4**, **5** and **6** were synthesized in the presence of the respective alkali metal halides.

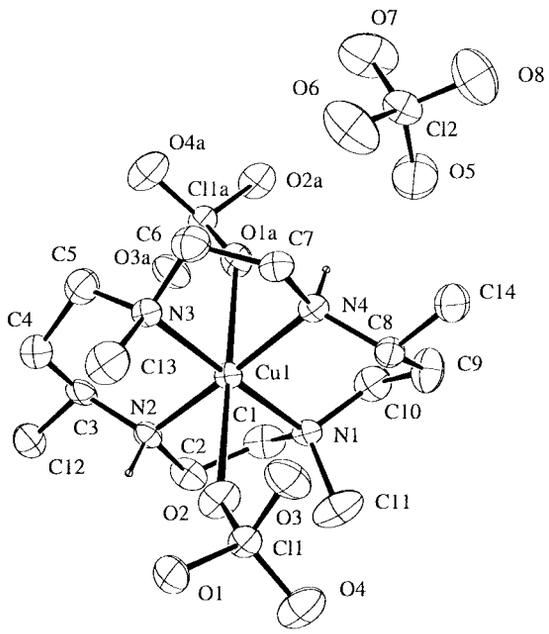

Fig. 1 An ORTEP drawing of the molecular structure of $[CuL^1(ClO_4)]ClO_4$ **1** along with the atom numbering scheme.

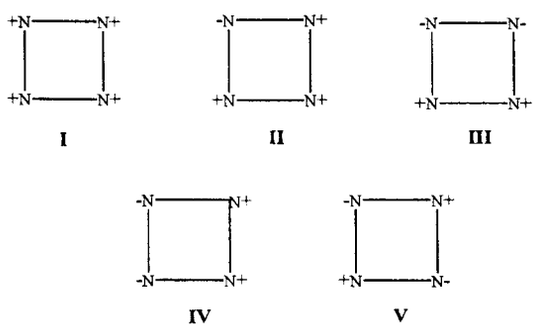

Fig. 2 Possible configurations of the cyclic ligand[15] (plus refers to a hydrogen that points above the plane and minus to one below).

Structures of complexes

$[CuL^1(ClO_4)]ClO_4$ 1. The structure of the complex showed the metal ion in six-co-ordinate geometry, involving two oxygen atoms of perchlorate groups in axial positions and four nitrogen atoms of the macrocycle in equatorial positions. One of the oxygen atoms comes from a perchlorate group of a symmetry related molecule, *i.e.* one perchlorate group co-ordinates two metal ions with two of its oxygen atoms, forming a linear chain. The other perchlorate group is not involved in co-ordination and is free in the lattice. The ORTEP[14] drawing of the complex is shown in Fig. 1 and selected bond lengths and bond angles are given in Table 2.

The macrocycle adapts the rare unstable *trans*-II stereochemistry according to the nomenclature of Bosnich *et al.*[15] (Fig. 2) where one six membered chelate ring is in unstable twisted form and one five membered ring is in eclipsed form. The other five and six membered chelate rings are in stable *gauche* and chair forms respectively. The average Cu–N (tertiary) bond length of 2.059(6) Å is longer than the average Cu–N (secondary) bond length (2.017(6) Å) and in the expected range. The average axial Cu–O (perchlorate) bond length (2.632(6) Å) is significantly lengthened making the geometry tetragonally elongated octahedral. This tetragonal distortion arises predominantly from the Jahn–Teller effect operative on the d^9 metal center.

Table 1 Crystallographic data for complexes $[CuL^1(ClO_4)]ClO_4$ **1**, $[CuL^1(N_3)_2]$ **2**, $[CuL^1(H_2O)_2][NO_2]_2$ **3**, $[CuL^1(H_2O)_2]Cl_2$ **4**, $[CuL^1(H_2O)_2]Br_2$ **5** and $[CuL^1(H_2O)_2]I_2$ **6**

	1	**2**	**3**	**4**	**5**	**6**
Chemical formula	$C_{14}H_{32}Cl_2CuN_4O_8$	$C_{14}H_{32}CuN_{10}$	$C_{14}H_{36}CuN_6O_6$	$C_{14}H_{36}Cl_2CuN_4O_2$	$C_{14}H_{36}Br_2CuN_4O_2$	$C_{14}H_{36}CuI_2N_4O_2$
M	518.88	404.04	448.03	426.91	515.83	609.81
Crystal system	Monoclinic	Monoclinic	Monoclinic	Monoclinic	Monoclinic	Monoclinic
Space group	$P2_1/n$	$P2_1/a$	$P2_1/n$	$P2_1/n$	$P2_1/n$	$P2_1/n$
a/Å	9.6358(1)	7.3939(1)	9.596(1)	8.973(1)	9.2448(8)	8.5634(3)
b/Å	14.5935(2)	16.1227(3)	12.157(1)	11.864(4)	12.115(2)	13.1899(5)
c/Å	15.1412(1)	8.5698(2)	9.698(1)	9.614(1)	9.749(1)	10.2121(4)
β/°	94.718(1)	114.381(1)	108.10(1)	106.93(2)	107.24(1)	103.266(1)
V/Å^3	2121.94(4)	930.50(3)	1075.4(2)	979.1(5)	1042.8(2)	1122.68(7)
Z	4	2	2	2	2	2
T/K	295	295	295	295	295	295
Reflections measured	12359	5049	1898	2846	3026	6408
Unique reflections	4636	1971	1898	2846	3026	2463
Observed reflections	3996	1490	1460	2336	1936	2285
R (on *F*)	11.03	3.96	4.59	3.13	11.4	2.75
R′ (on F^2)	28.65	10.04	13.42	8.31	52.70	6.06

Table 2 Selected bond lengths (Å) and angles (°) in $[CuL^1(ClO_4)]ClO_4$ **1** and $[CuL^1(N_3)_2]$ **2**

$[CuL^1(ClO_4)]ClO_4$ **1**			
Cu–N(1)	2.057(6)	Cu–N(2)	2.016(6)
Cu–N(3)	2.061(6)	Cu–N(4)	2.019(6)
Cu–O(1A)	2.698(5)	Cu–O(2)	2.566(5)
N(1)–Cu–N(2)	86.7(3)	N(3)–Cu–N(4)	85.7(2)
N(1)–Cu–N(3)	178.4(2)	N(2)–Cu–N(4)	176.1(2)
N(1)–Cu–O(2)	89.6(3)	N(2)–Cu–O(2)	82.1(2)
N(3)–Cu–O(2)	91.7(2)	N(4)–Cu–O(2)	101.8(2)
O(2)–Cu–O(1A)	178.1(2)		
$[CuL^1(N_3)_2]$ **2**			
Cu–N(1)	2.090(2)	Cu–N(2)	2.045(2)
Cu–N(3)	2.504(1)		
N(1)–Cu–N(2)	86.7(3)	N(2)–Cu–N(1′)	93.3(1)
N(1)–Cu–N(1′)	180.0	N(2)–Cu–N(2′)	180.0
N(3)–Cu–N(1)	94.3(1)	N(3)–Cu–N(2)	93.4(1)
N(3)–Cu–N(3′)	180.0		

Primed atoms are related by the symmetry transformation $-x, -y, -z$.

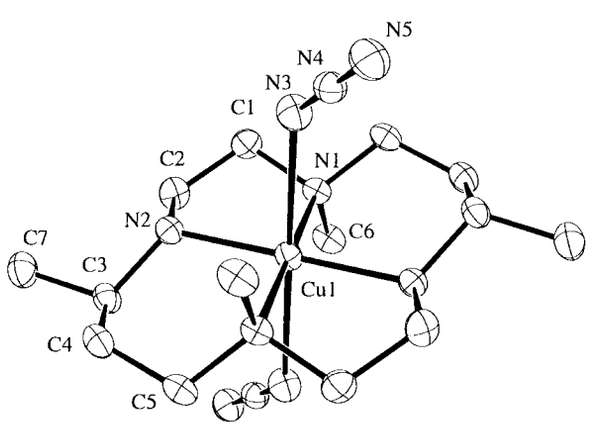

Fig. 3 An ORTEP drawing of the molecular structure of $[CuL^1(N_3)_2]$ **2**.

The structure of the blue isomer differs from that of the red isomer in the configuration at one chiral nitrogen center, as is confirmed by comparison of the two crystal structures. The structure of the red isomer (reported by our group recently[8]) showed two molecules with different disordered configurations with 0.5 occupancy in a unit cell. The macrocycle adapted the stable *trans*-III configuration in both molecules where all the four chelate rings are in the stable form. The two molecules

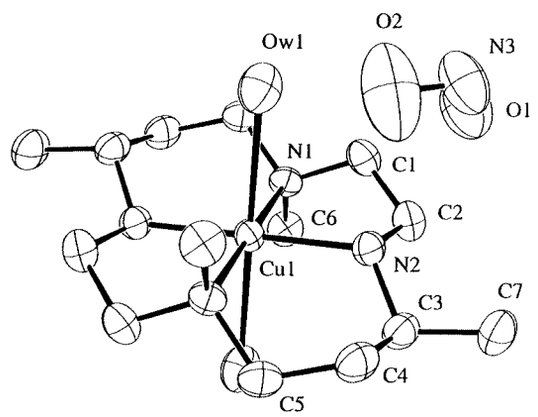

Fig. 4 An ORTEP drawing of the molecular structure of $[CuL^1(H_2O)_2][NO_2]_2$ **3**.

are diastereomers as the only significant difference was the orientation of the *C*-methyl groups that were axial in one and equatorial in the other molecule.

$[CuL^1(N_3)_2]$ 2. The structure of this complex (Fig. 3) showed the macrocyclic ligand in stable *trans*-III configuration.[15] The metal ion is co-ordinated by two azide nitrogen atoms in axial positions and the four nitrogen atoms of the macrocycle in the equatorial positions. The axial Cu–N bonds (2.504 Å) are once again elongated making the geometry tetragonally elongated octahedral. The bond lengths and angles are typical of tetraaza macrocyclic complexes and are presented in Table 2.

$[CuL^1(H_2O)_2][NO_2]_2$ 3, $[CuL^1(H_2O)_2]Cl_2$ 4, $[CuL^1(H_2O)_2]Br_2$ 5 and $[CuL^1(H_2O)_2]I_2$ 6. All these complexes crystallized in the same space group $P2_1/n$ and are isomorphous. The structures (Figs. 4–7) showed the cations on a center of symmetry. The macrocyclic ligand adapted the stable *trans*-III configuration[15] with the two six membered chelate rings in the chair form and the two five membered rings in the *gauche* form. The two *C*-methyl groups are also in the stable equatorial positions. The Cu–N bonds lengths are within the average equatorial Cu–N distances of 2.03(3) Å for copper(II) macrocyclic compounds.[16] The N–Cu–N bond angles are also in the expected range (Table 3). The axial Cu–O (H_2O) bonds are significantly lengthened and the geometry is described as tetragonally elongated octahedral.

The two hydrogen atoms of the water molecule are involved in hydrogen bonding where one is bonded to the halide ion, the other to the halide ion of a symmetry related molecule. The amine hydrogen atoms are also hydrogen bonded to the

Table 3 Selected bond lengths (Å) and angles (°) in $[CuL^1(H_2O)_2][NO_2]_2$ **3**, $[CuL^1(H_2O)_2]Cl_2$ **4**, $[CuL^1(H_2O)_2]Br_2$ **5** and $[CuL^1(H_2O)_2]I_2$ **6**

	3	4	5	6
Cu–N(1)	2.050(3)	2.055(2)	2.054(2)	2.045(2)
Cu–N(2)	2.031(3)	2.032(2)	2.037(2)	2.041(2)
Cu–OW(1)	2.624(3)	2.692(2)	2.695(2)	2.725(3)
N(1)–Cu–N(2)	86.4(1)	86.5(1)	86.1(7)	86.5(1)
N(1)–Cu–N(1′)	180.0	180.0	180.0	180.0
N(1)–Cu–OW(1)	85.2(1)	85.2(1)	84.1(7)	85.1(1)
N(2)–Cu–N(1′)	93.6(1)	93.5(1)	93.9(1)	93.5(1)
N(2)–Cu–N(2′)	180.0	180.0	180.0	180.0
N(2)–Cu–OW(1)	86.6(1)	88.8(1)	89.3(1)	88.1(1)
OW(1)–Cu–OW(1′)	180.0	180.0	180.0	180.0

Primed atoms are related by the symmetry transformation $-x, -y, -z$.

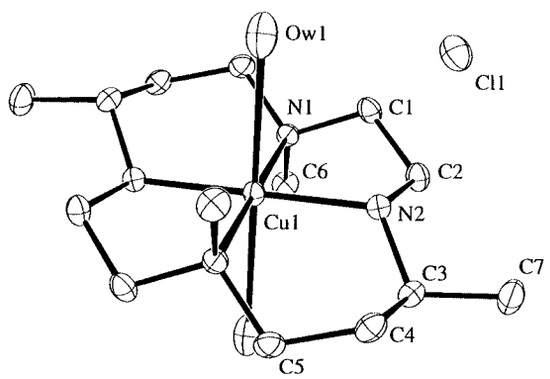

Fig. 5 An ORTEP drawing of the molecular structure of $[CuL^1(H_2O)_2]Cl_2$ **4**.

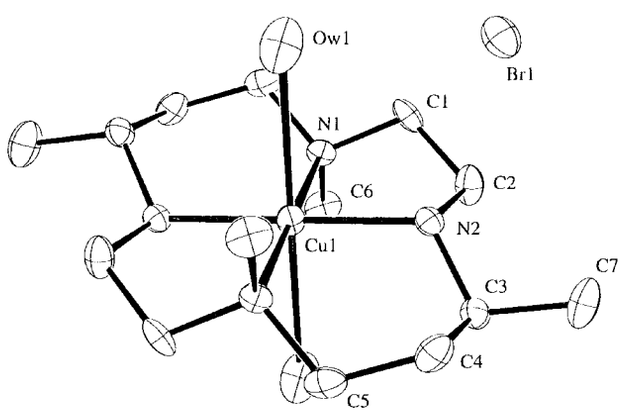

Fig. 6 An ORTEP drawing of the molecular structure of $[CuL^1(H_2O)_2]Br_2$ **5**.

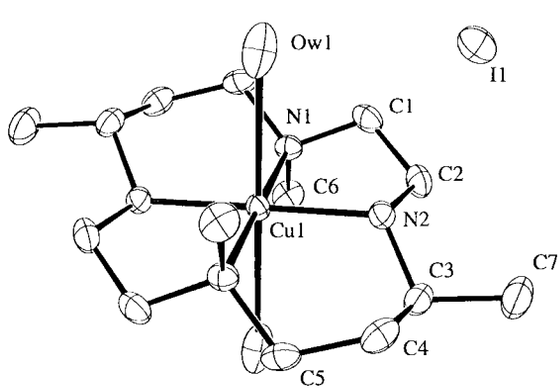

Fig. 7 An ORTEP drawing of the molecular structure of $[CuL^1(H_2O)_2]I_2$ **6**.

Table 4 Electronic spectral and cyclic voltammetric data

Complex	λ_{max}/nm (ε/M^{-1} cm^{-1})	$E_{\frac{1}{2}}$/V for Cu^{II}–Cu^{I} [a]
$[CuL^1(ClO_4)]ClO_4$ (blue)	540 (216) [b]	−0.55
	545 (177) [c]	
	538 (147) [d]	
$[CuL^1(ClO_4)_2]$ (red)	523 (165) [b]	−0.70
	524 (171) [c]	
	519 (130) [d]	
$[CuL^1(N_3)_2]$	591 (135) [b]	−0.96
$[CuL^1(H_2O)_2][NO_2]_2$	552 (138) [b]	−0.76
$[CuL^1(H_2O)_2]Cl_2$	592 (269) [b]	−0.76
$[CuL^1(H_2O)_2]Br_2$	579 (252) [b]	−0.77
$[CuL^1(H_2O)_2]I_2$	549 (182) [b]	−0.75

[a] In CH_3CN at 298 K (scan rate = 100 mV s^{-1}) using 0.1 M NBu_4ClO_4 as supporting electrolyte at a platinum working electrode with Ag–AgCl as reference electrode. [b] In acetonitrile. [c] In water. [d] In 5.0 M $NaNO_3$ solution.

halide ion. The molecules form linear chains through hydrogen bonding. In complex **3** both the amine hydrogen atoms and those of the water molecule are involved in hydrogen bonding with the oxygen atoms of the NO_2 group.

Spectral and redox studies

The electronic spectra of these complexes showed broad bands in the range 520 to 590 nm. This region is close to those of square planar complexes.[17] This is due to the Jahn–Teller distortion operating in the d^9 systems that is also confirmed from the structures which show significantly elongated axial bond distances compared to the relatively shorter equatorial Cu–N bonds. The electronic spectral data are given in Table 4.

Cyclic voltammetric experiments were carried out in acetonitrile solvent at a platinum electrode. All the complexes showed single quasireversible to irreversible couples corresponding to reduction of Cu^{II} to Cu^{I} (Table 4). Complex **1** (blue isomer) exhibited a quasireversible wave at −0.55 V while the red isomer exhibited it at −0.70 V. The copper(II) oxidation state is relatively stabilized in the red isomer due to the planar configuration of the macrocycle. In other words, the macrocycle with two unstable chelate rings in the blue isomer destabilizes the copper(II) oxidation state by almost 150 mV. The redox processes in complexes **3**, **4**, **5** and **6** were observed at almost similar potentials at ≈−0.76 V due to similar structures. The copper(II) oxidation state is highly stabilized in complex **2** (−0.96 V) due to the electron donating azide group co-ordinating in the axial positions.

Kinetic studies

The dissociation kinetics of complex **1** was studied in HNO_3–$NaNO_3$ aqueous solutions in the temperature range 25.0 ± 0.1 to 45.0 ± 0.1 °C (I = 5.0 M). Under these conditions the reactions were found to go to completion. The dissociation occurred in a single stage with the rate equation (1). An isos-

$$-d[CuL^{2+}]/dt = k_{obs}[CuL^{2+}] \quad (1)$$

bestic point was observed at 760 nm (SUP 57621). No significant amount of intermediate was formed in the solution and the complex dissociated with the observed pseudo first-order rate constants k_{obs} showing an acid dependence. The values of k_{obs} as a function of acid concentration and temperature are given in Table 5.

Plots of k_{obs} *vs.* $[H^+]$ are linear (Fig. 8) and the reaction obeys the simple rate equation (2). The value of k_{1H} obtained from the

$$k_{obs} = k_{1H}[H^+] + k_{1d} \quad (2)$$

Table 5 Pseudo first order rate constants for acid catalysed dissociation of $[CuL^1(ClO)_4]ClO_4$ **1** at $I = 5.0$ M (HNO_3 + $NaNO_3$) as a function of acid concentration

	$10^4\ k_{obs}/s^{-1}$				
$[HNO_3]$/M	25 ± 0.1	30 ± 0.1	35 ± 0.1	40 ± 0.1	45 ± 0.1 °C
1.00	0.77	1.04	1.38	1.81	2.70
2.00	1.13	1.46	2.15	2.88	4.03
3.00	1.38	1.84	2.73	3.79	5.34
4.00	1.63	2.24	3.27	4.61	7.12
5.00	1.86	2.52	3.74	5.61	8.23

Table 6 Temperature dependence of the acid catalyzed dissociation of $[CuL^1(ClO)_4]ClO_4$ **1**

T/°C	$10^5\ k$/M^{-1} s^{-1}	$10^5\ k_d$/s^{-1}	kk_d^{-1}/M^{-1}
25	2.66	5.54	0.48
30	3.74	6.98	0.54
35	5.84	9.01	0.65
40	9.33	9.43	0.99
45	14.16	12.33	1.15

For k_{1H}: $\Delta H^{\ddagger}_{1H} = 64.7$ kJ mol^{-1} and $\Delta S^{\ddagger}_{1H} = -117$ J K^{-1} mol^{-1}. For k_d: $\Delta H^{\ddagger}_{1d} = 27.4$ kJ mol^{-1} and $\Delta S^{\ddagger}_{1d} = -234$ J K mol^{-1}.

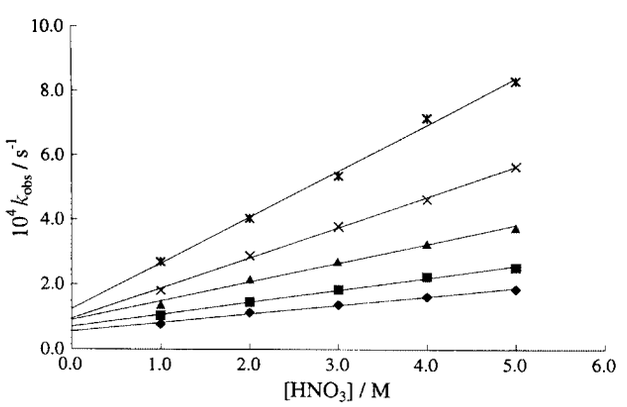

Fig. 8 Plots of k_{obs} *vs.* [H$^+$] for the dissociation of complex **1** at $I = 5.0$ M (HNO_3–$NaNO_3$) in the temperature range 25.0–45.0 °C (◆–*). The points are the experimental results; the lines are calculated from $k_{obs} = k_{23}K_{12}[H^+] + k_{24}K_{12}$ where $k_{23}K_{12}$ is 2.66×10^{-5} M^{-1} s^{-1} and $k_{24}K_{12}$ is 5.54×10^{-5} s^{-1} at 25.0 ± 0.1 °C.

slope of the plot is 2.66×10^{-5} M^{-1} s^{-1} and the value of k_{1d} from the intercept is 5.54×10^{-5} s^{-1} at 25.0 ± 0.1 °C. The ratio $k_{1H}:k_{1d}$ is 0.48 M^{-1}. The proposed mechanism of dissociation is shown in Scheme 1. The experimental equation (2) is consistent with the mechanism in eqns. (3)–(7). For this mechanism the

$$\mathbf{i} \overset{K_{12}}{\rightleftharpoons} \mathbf{ii} \quad (3)$$

$$\mathbf{ii} + H^+ \xrightarrow{k_{23}} \mathbf{iii} \quad (4)$$

$$\mathbf{iii} \xrightarrow{\text{fast}} \text{products} \quad (5)$$

$$\mathbf{ii} + \text{solv} \xrightarrow{k_{24}} \mathbf{iv} \quad (6)$$

$$\mathbf{iv} \xrightarrow{\text{fast}} \text{products} \quad (7)$$

rate equation $k_{obs} = k_{23}K_{12}[H^+] + k_{24}K_{12}$ holds good, where $k_{23}K_{12}$ is k_{1H} and $k_{24}K_{12}$ is k_{1d}.

The temperature dependence of k_{1H} (Table 6) gives $\Delta H^{\ddagger}_{1H} = 64.7$ kJ mol^{-1} and $\Delta S^{\ddagger}_{1H} = -117$ J K^{-1} mol^{-1} while

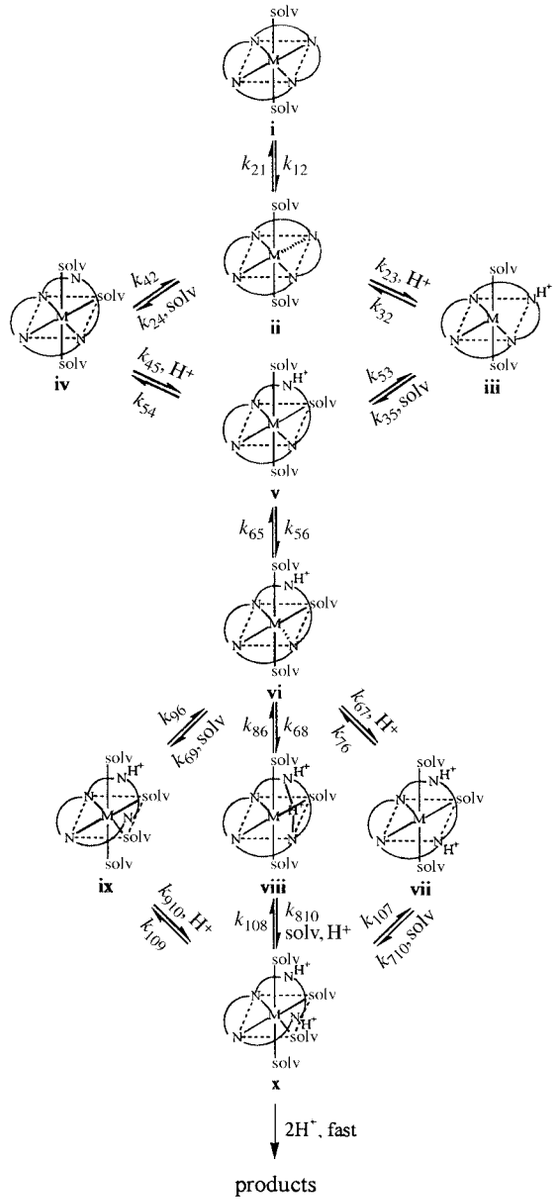

Scheme 1 Proposed mechanism for the acid catalyzed dissociation of macrocyclic complexes (solv = solvent).

for k_{1d} the parameters are $\Delta H^{\ddagger}_{1d} = 27.4$ kJ mol^{-1} and $\Delta S_{1d}{}^{\ddagger} = -234$ J K^{-1} mol^{-1}. The very large negative values for the entropy of activation for the solvation pathway (k_{1d}) presumably reflects the high degree of solvent reorganization required in the transition state of the reaction. It is interesting that both the enthalpy of activation and entropy of activation for the protonation pathway (k_{1H}) are much larger than those for the solvation pathway. The relatively large $\Delta H^{\ddagger}_{1H}$ and $\Delta S^{\ddagger}_{1H}$ are mainly due to the desolvation of the proton in the protonation pathway.

Dissociation kinetics of a few copper(II) complexes of macrocyclic tetraamine complexes has been studied at 25.0 ± 0.1 °C with $I = 5.0$ M (HNO_3 + $NaNO_3$).[2–5,18] In marked contrast to the behavior of $[CuL^1(ClO_4)]ClO_4$, these complex ions exhibited consecutive processes with reversible steps as given in eqn. (8). The kinetic results for these reactions can

$$[CuL]^{2+} \underset{k_{-1}}{\overset{k_1}{\rightleftharpoons}} [Cu(HL)]^{3+} \xrightarrow{k_2} Cu^{2+} + H_4L^{4+} \quad (8)$$

readily be explained by the mechanism presented in Scheme 1. The measured and the corresponding mechanistic rate constants are listed in Table 7.

Table 7 Rate constants for dissociation of copper(II) macrocyclic tetraamine complexes at 25.0 ± 0.1 °C and I = 5.0 M (HNO_3 + $NaNO_3$)

Measured rate constant	Mechanistic rate constant	**1**	[Cu(cyclam)]$^{2+}$	[Cu(tet-a)]$^{2+}$ (blue)	[Cu(tet-a)]$^{2+}$ (red)	[Cu(tet-b)]$^{2+}$ (blue)	[Cu(tet-b)]$^{2+}$ (red)
k_{1H}/M^{-1} s^{-1}	$k_{12}\,k_{23}/k_{21}$	2.66×10^{-5}	3.15×10^{-4}	2.60×10^{-4}	2.27×10^{-8}	1.42×10^{-6}	3.06×10^{-7}
k_{1d}/s^{-1}	$k_{12}\,k_{24}/k_{21}$	5.54×10^{-5}				5.20×10^{-7}	1.08×10^{-7}
k_{-1H}/s^{-1}	$k_{32}\,k_{53}/k_{35}$		2.76×10^{-3}	1.40×10^{-3}	2.52×10^{-3}	2.80×10^{-6}	1.32×10^{-5}
k_{-1d}/M^{-1} s^{-1}	$k_{42}\,k_{54}/k_{45}$					1.10×10^{-6}	9.98×10^{-6}
k_{2H}/M^{-1} s^{-1}	$k_{56}\,k_{67}/k_{65}$		4.91×10^{-5}	1.05×10^{-5}	1.03×10^{-5}	1.70×10^{-6}	3.14×10^{-7}
k_{2d}/s^{-1}	$k_{56}\,k_{69}/k_{96} + k_{56}\,k_{68}/k_{86}$		5.10×10^{-4}	4.60×10^{-4}	4.46×10^{-4}	1.15×10^{-5}	2.56×10^{-6}
Ref.		This work	18	2	4	3	5

Table 8 Selected structural data for copper(II) macrocyclic tetraamine complexes

	1	[Cu(cyclam)]$^{2+}$	[Cu(tet-a)]$^{2+}$ (blue)[a]	[Cu(tet-a)]$^{2+}$ (red)	[Cu(tet-b)]$^{2+}$ (blue)	[Cu(tet-b)]$^{2+}$ (red)
Cu–N/Å	2.016(6); 2.019(6) 2.057(6); 2.061(6)	2.02(2) 2.02(4)		2.022(2) 2.063(3)	1.99(2) 2.06(2)	1.992(3) 2.000(3)
Chelate angle for five membered ring/°	85.7(2) 86.7(3)	86.0(2)		85.7(1)	85.0(3)	88.5(1)
Chelate angle for six membered ring/°	93.1(3) 94.5(3)	94.0(2)			95.4(3)	93.4(1)
N–Cu–N *trans* angle/°	176.1(2) 178.4(2)					159.4(1) 169.2(1)
Conformation of chelate rings	*gauche*; eclipsed chair; twist	*gauche*; *gauche* chair; chair	*gauche*; eclipsed chair; twist	*gauche*; *gauche* chair; chair	*gauche*; *gauche* chair; chair	twist; twist chair; chair
Co-ordination number	6	6	6	6	5	5
Ref.	This work	22	19	19	20	21

[a] No clear structural parameters were given as the structure could not be refined completely. However octahedral geometry was assigned based on these data and spectral studies.

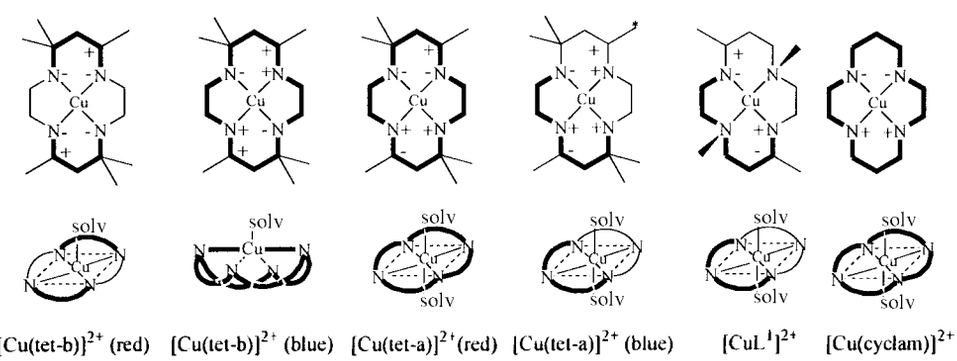

Fig. 9 Conformations of the chelate rings and configurations at the asymmetric center for some copper(II) macrocyclic complexes. The plus and minus signs indicate the position of the hydrogen atom above and below the plane of the macrocycle respectively. The *gauche* and chair conformations of the five and six membered chelate rings are indicated by heavier lines. The axial C(7) methyl group is indicated by an asterisk.

Mechanistic interpretation

Based on the data in Table 7, the following preliminary observations are particularly noteworthy. (1) Dissociation of [CuL^1-(ClO$_4$)]ClO$_4$, **1** differs quite markedly from the other 14-membered macrocyclic tetraamine complexes. It was found to occur by a single state, indicating that cleavage of the first Cu–N bond is rate determining. In contrast, the rate determining step for each of the other complexes in Table 7 is cleavage of the second Cu–N bond. (2) The cleavage of the first Cu–N bond of [Cu(cyclam)]$^{2+}$, [Cu(tet-a)]$^{2+}$ (red) (tet-a = C-*meso*-5,5,7,12,12,14-hexamethyl-1,4,8,11-tetraazacyclotetradecane) and [Cu(tet-a)]$^{2+}$ (blue) is dominantly *via* the protonation pathway, while in the cleavage of the first Cu–N bond of [Cu(tet-b)]$^{2+}$ (red) (tet-b = C-*rac*-5,5,7,12,12,14-hexamethyl-1,4,8,11-tetraazacyclotetradecane) and [Cu(tet-b)]$^{2+}$ (blue) both protonation and solvation pathways make a significant contribution. (3) The rates of these reactions are very sensitive to the structures of these complexes. The values of k_{1H} increases in the order [Cu(tet-a)]$^{2+}$ (red) < [Cu(tet-b)]$^{2+}$ (red) < [Cu(tet-b)]$^{2+}$ (blue) < [CuL^1]$^{2+}$ **1** < [Cu(tet-a)]$^{2+}$ (blue) < [Cu(cyclam)]$^{2+}$. The implications of these observations are examined in detail below.

As seen from the crystal structure of [CuL^1(ClO$_4$)]ClO$_4$ one six membered and one five membered chelate ring are in the unstable configuration. The Cu–N (tertiary) bond of these two unstable chelate rings is longer than the other Cu–N bonds and is expected to be easy to break. After breaking this bond the macrocyclic ligand twists and folds, the *N*-methyl groups hinder the recombination of the Cu–N bond and accelerate cleavage of the Cu–N bond with the result that k_{-1} is smaller than k_2 in eqn. (8). Therefore, the cleavage of the first Cu–N bond becomes rate determining.

For dissociation of five-co-ordinate complexes both the solvation and the protonation pathways make a contribution to the rate, whereas for dissociation of six-co-ordinate complexes the protonation pathway is much more important than the solvation pathway. The complex $[CuL^1(ClO_4)]ClO_4$ **1** is the only exception to this rule. This difference in behavior of **1** is due to the steric hindrance of the methyl groups on the nitrogen atoms of the macrocycle which inhibit protonation of the nitrogen atoms. Thus dissociation by the solvation and protonation pathways is equally important.

The important factors affecting the rate constant k_{1H} are: number of methyl groups, ligand field activation energy (LFAE), conformation of the chelate rings and position of the methyl groups (axial or equatorial). The steric effect of the methyl groups hinders the dissociation of these macrocyclic complexes to a very large extent, thus the rate decreases with increase in the number of methyl groups. The relatively large k_{1H} of $[Cu(cyclam)]^{2+}$ is mainly due to this effect.

The crystal structures[19–22] and the ligand field spectra[2–5] for all these complexes have been reported. Selected structural data of these complexes are given in Table 8.[19–22] The configurations at the asymmetric center and the conformations of the chelate rings are shown in Fig. 9. Based on this information, we expect the LFAE to decrease in the order $[Cu(cyclam)]^{2+} > [Cu(tet\text{-}a)]^{2+}$ (red) $> [Cu(tet\text{-}b)]^{2+}$ (red) $> [CuL^1]^{2+} > [Cu(tet\text{-}a)]^{2+}$ (blue) $> [Cu(tet\text{-}b)]^{2+}$ (blue) and the conformational energies increase in the order $[Cu(cyclam)]^{2+} < [Cu(tet\text{-}a)]^{2+}$ (red) $< [Cu(tet\text{-}b)]^{2+}$ (blue) $< [Cu(tet\text{-}b)]^{2+}$ (red) $< [CuL^1]^{2+}$, **1** $< [Cu(tet\text{-}a)]^{2+}$ (blue).

The position of the methyl groups plays an important role in the dissociation kinetics of these complexes. The equatorial methyl groups strongly inhibit the reaction, while the axial methyl groups accelerate the rate. The relatively large k_{1H} for the reaction of $[Cu(tet\text{-}a)]^{2+}$ (blue) is mainly due to the presence of two methyl groups in the unstable axial positions on the six membered chelate rings as shown in Fig. 9. The order of k_{1H}, $[Cu(tet\text{-}a)]^{2+}$ (red) $< [Cu(tet\text{-}b)]^{2+}$ (red) $< [Cu(tet\text{-}b)]^{2+}$ (blue) $< [CuL^1]^{2+}$ **1** $< [Cu(tet\text{-}a)]^{2+}$ (blue) $< [Cu(cyclam)]^{2+}$, is a combined effect of these four factors.

Acknowledgements

Financial support from National Science Council (NSC), Taiwan, ROC under grants NSC88-2112-M007-013 and NSC88-2113-M007-013 is gratefully acknowledged. H. A. and K. P. thank NSC for Postdoctoral Fellowships.

References

1 G. Melson (Editor), *Coordination Chemistry of Macrocyclic compounds*, Plenum, New York, 1979; P. V. Bernhardt and G. A. Lawrance, *Coord. Chem. Rev.*, 1990, **104**, 297; K. P. Wainwright, *Coord. Chem. Rev.*, 1997, **166**, 35.
2 B. F. Liang and C. S. Chung, *Inorg. Chem.*, 1981, **20**, 2152.
3 B. F. Liang and C. S. Chung, *Inorg. Chem.*, 1983, **22**, 1017.
4 J.-W. Chen, D.-S. Wu and C.-S. Chung, *Inorg. Chem.*, 1986, **25**, 1940.
5 L.-H. Chen and C.-S. Chung, *J. Chin. Chem. Soc.*, 1989, **36**, 195.
6 K. Miyamura, M. Kohzuki, R. Narushima, M. Saburi, Y. Gohshi, S. Tsuboyama and T. Sakurai, *J. Chem. Soc.*, *Dalton Trans.*, 1987, 3093.
7 D. D. Perrin, W. L. F. Armarego and D. R. Perrin, *Purification of Laboratory Chemicals*, Pergamon, London, 1980.
8 K. Panneerselvam, T.-H. Lu, S.-F. Tung, T.-Y. Chi, C. Pariya and C.-S. Chung, *Anal. Sci.*, 1998, **14**, 1031.
9 A. C. T. North, D. C. Phillips and F. S. Mathews, *Acta Crystallogr.*, *Sect. A*, 1968, **24**, 351.
10 G. M. Sheldrick, SHELXTL PLUS, Siemens Anaytical X-Ray Instruments Inc., Madison, WI, 1990.
11 E. J. Gabe, Y. Le Page, J.-P. Charland, F. L. Lee and P. S. White, *J. Appl. Crystallogr.*, 1989, **22**, 384.
12 G. M. Sheldrick, *Acta Crystallogr.*, *Sect. A*, 1990, **46**, 467.
13 G. M. Sheldrick, SHELXL 97, Program for refinement of crystal structures, University of Göttingen, 1997.
14 C. K. Johnson, ORTEP II, Report ORNL-5138, Oak Ridge National Laboratory, Oak Ridge, TN, 1976.
15 B. Bosnich, C. K. Poon and M. Tobe, *Inorg. Chem.*, 1965, **4**, 1102.
16 T.-H. Lu, C.-S. Chung, T. Ashida, *J. Chin. Chem. Soc.* (*Taipei*), 1991, **38**, 147.
17 J. Chapman, G. Ferguson, J. F. Gallagher, M. C. Jennings and D. Parker, *J. Chem. Soc.*, *Dalton Trans.*, 1992, 345.
18 L.-H. Chen and C.-S. Chung, *Inorg. Chem.*, 1988, **27**, 1880.
19 R. Clay, J. Murray-Rust and P. Murray-Rust, *J. Chem. Soc.*, *Dalton Trans.*, 1979, 1135.
20 T.-J. Lee, H. Y. J. Lee, C.-S. Lee and C.-S. Chung, *Acta Crystallogr.*, *Sect. C*, 1984, **40**, 641.
21 T.-H. Lu, W.-C. Liang, D.-T. Wu and C.-S. Chung, *Acta Crystallogr.*, *Sect. C.*, 1986, **42**, 801.
22 P. A. Tasker and L. Sklar, *J. Cryst. Mol. Struct.*, 1975, **5**, 329.

Paper 9/05079E